Identification of XV-15 Aeroelastic Modes Using Frequency Sweeps

C. W. Acree Jr.*
NASA Ames Research Center, Moffett Field, California
and
Mark B. Tischler†
U. S. Army Aviation Research and Technology Activity, Moffett Field, California

The XV-15 tilt-rotor wing has six major aeroelastic modes that are close in frequency. To precisely excite individual modes during flight test, dual flaperon exciters with automatic frequency-sweep controls were installed. The resulting structural data were analyzed in the frequency domain (Fourier-transformed). Modal frequencies and damping were determined by performing curve fits to frequency-response magnitude and phase data. Results are given for the XV-15 with its original metal rotor blades. Frequency and damping values are also compared with predictions by two different programs, CAMRAD and ASAP.

Introduction

DISTINCTIVE features of the XV-15 tilt rotor (Fig. 1) are the large wing-tip pylons that house the engines, transmissions, and pivoting mechanisms for each rotor. The concentrated masses at the wing tips keep the modal frequencies fairly low. Also, aeroelastic coupling between each rotor and pylon is destabilizing. Consequently, close attention must be paid to potential whirl-mode flutter during flight test. The highest speeds are attained in the cruise mode (pylons down), making it the critical operating mode for aeroelastic stability. The problem is not unique to the XV-15 research aircraft, but is fundamental to any tilt rotor aircraft of similar configuration, such as the XV-3, for which extensive studies were done,[1,2] and the upcoming V-22 Osprey.[3]

A thorough re-evaluation of XV-15 aeroelastics with the existing metal rotor blades was conducted in preparation for flight tests of new composite blades.[4] A critical requirement was to validate the new modal identification techniques within the existing XV-15 flight envelope before flying the new advanced technology blades (ATB's). Accordingly, all flight-test data discussed herein are for the metal blades.

The XV-15 wing modes were excited with flaperon frequency sweeps, and frequency spectra of the resulting time-history data were generated with chirp z-transforms. Modal frequencies and damping were determined by performing curve fits to frequency-response magnitude and phase data. In addition to the flight-data analyses, two different theoretical analyses, CAMRAD and ASAP, were employed to predict the modes using mathematical models of the XV-15.

Early results of the frequency-domain analysis are reported in Ref. 5, along with modal predictions. Both the flight-test data analysis and the predictive programs were subsequently revised, sometimes extensively. The updated results are given herein. More general overviews of XV-15 structural dynamics, including previous flight-test data, are given in Refs. 6 and 7.

This report presents discussions of the XV-15 aeroelastic modes and the flight-test techniques used to excite them; the analytical procedures used to extract modal frequencies and damping from flight-test data; and the plots of estimated frequency and damping vs airspeed, including comparisons with values predicted by both CAMRAD and ASAP.

Received Dec. 17, 1987; revision received Jan. 12, 1989.

*Aerospace Engineer. Member AIAA.
†Research Scientist, Aeroflightdynamics Directorate. Member AIAA.

Flight-Test Methods

The intent of the flight tests was to validate the frequency-domain modal identification method and to map out the dominant aeroelastic modes, which are illustrated in Fig. 2 along with the values of structural frequencies f_s and damping ζ_s used for all predictions given herein. As will be shown, some predictions were inaccurate even though they include refinements made after the aircraft was initially tested.

For certain combinations of altitude, rotor speed, and power, at least one mode is predicted to become unstable at a sufficiently high airspeed. Also, the symmetric torsion mode lies within the design rotor-speed range. Consequently, the rotor speed with the metal blades is restricted in cruise to 8.6 Hz (86% of 601 rpm) instead of the design minimum of 7.6 Hz. Except for the symmetric beam mode, all modes lie within about 2 Hz of each other; two – the antisymmetric chord and antisymmetric torsion modes – are within 0.1 Hz at low airspeeds. The predicted instability and restricted rotor-speed range make precise identification of individual modes neces-

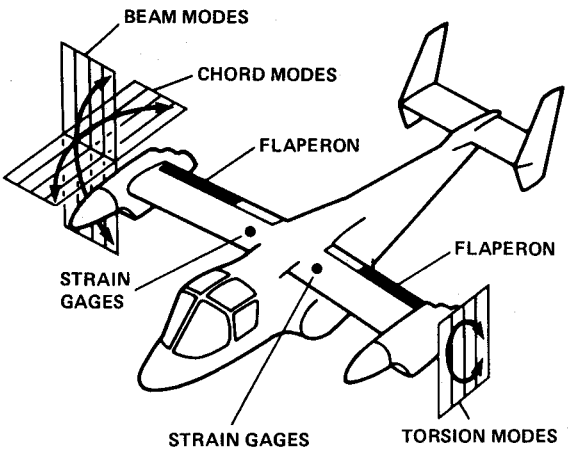

Fig. 1 XV-15 in cruise mode, showing flaperons, strain gage locations, and wing modes.

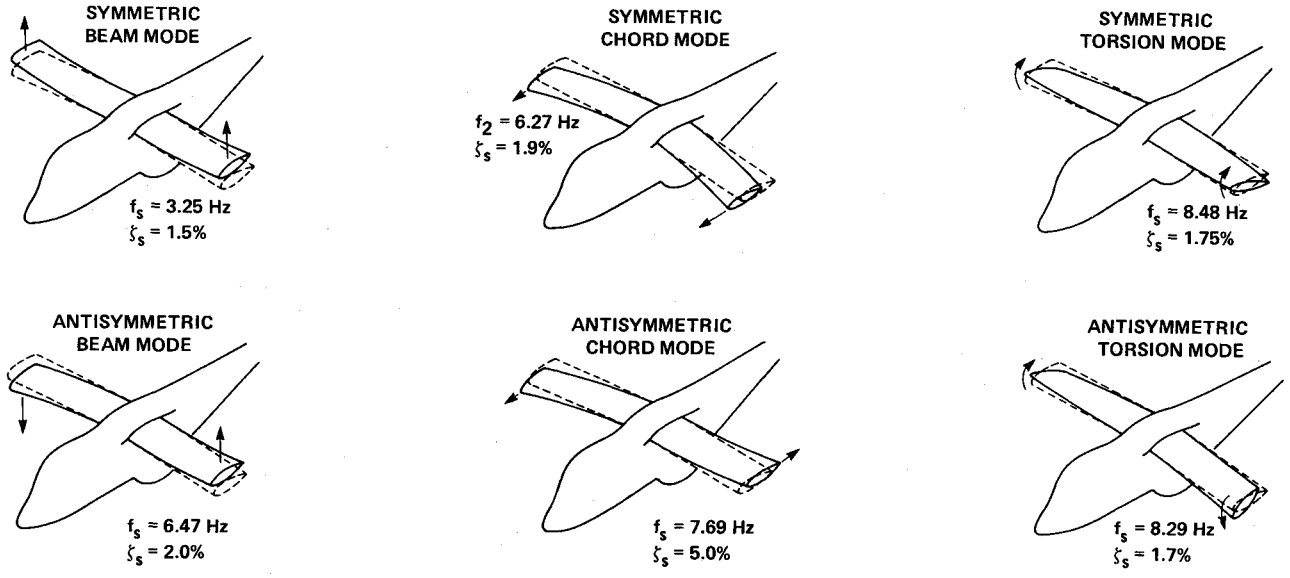

Fig. 2 XV-15 wing modes, with structural frequencies and damping.

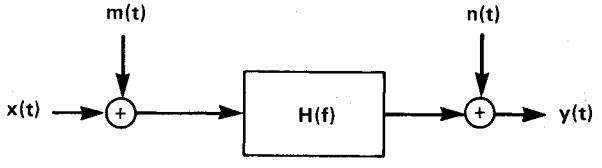

Fig. 3 Signals and noise affecting frequency-response calculations.

sary, and the close placement in frequency makes such identification difficult.

In earlier flight tests,[6,7] frequency and damping were identified by a variety of techniques, primarily exponential decays with Prony analysis, and (limited) turbulence excitation with RANDOMDEC and frequency-domain analyses, all with marginally acceptable results. Compared to such techniques, the frequency-sweep method is less sensitive to noise and requires less flight time, making it the method of choice. (Reference 6 lists the pros and cons of the different flight-test techniques, and Refs. 8 and 9 discuss the limiting errors of the associated analytical methods.)

High-frequency, limited-authority servo actuators in series with the flaperon control linkages excited the modes. Symmetric modes were excited by driving the left and right flaperons in phase; antisymmetric modes were excited by driving the flaperons in opposite phase. An amplitude of 100% equaled ± 5 deg of flaperon motion.

An electronic controller automatically swept the flaperons from 1 to 10 Hz, using a logarithmically increasing sweep rate of approximately 10 cycles per octave (the sweep rate was proportional to frequency). This was faster than the rate recommended in Ref. 10, but still slow enough to clearly reveal each mode. Three such sweeps in succession were performed at each test condition.

Analysis Methods

The overall concept of the modal indentification method used in this study is to first estimate the frequency response $H(f)$ between the aircraft excitation and structural response, and then to determine the modal damping and frequency by second-order model fitting.

Figure 3 illustrates the excitation of the aircraft by measurable and unmeasurable inputs $x(t)$ and $m(t)$; the measured response $y(t)$ is corrupted by measurement noise $n(t)$. If the measurable and unmeasurable inputs and measurement noise are fully uncorrelated, then the unbiased (true average value)

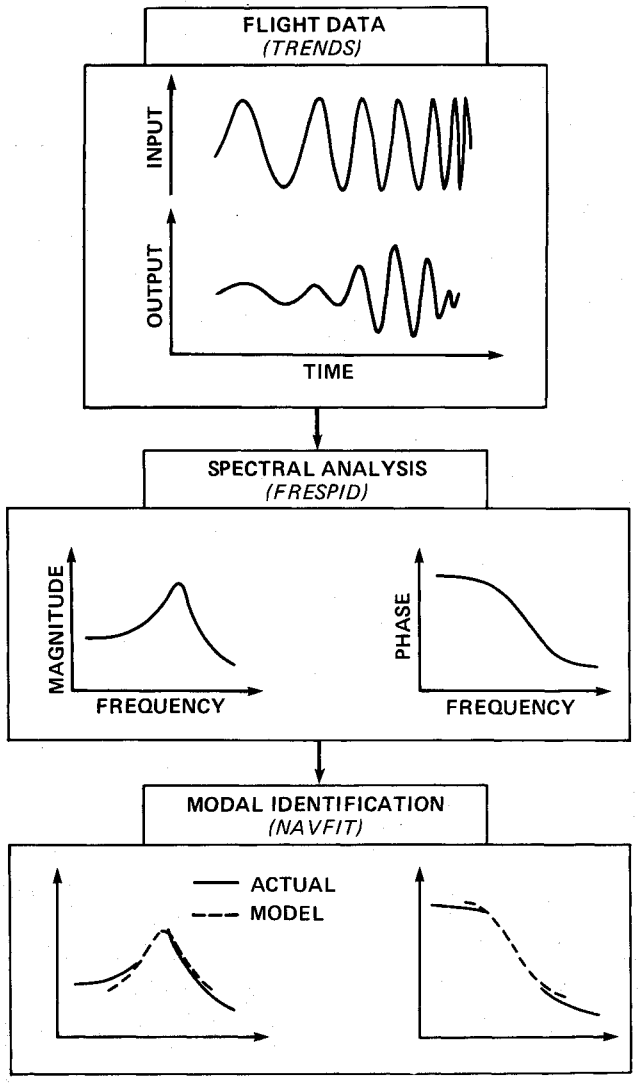

Fig. 4 Data processing for frequency-domain modal identification.

frequency response $H(f)$ may be estimated from the cross- and auto-spectral functions $G_{xy}(f)$ and $G_{xx}(f)$ as[9]

$$\hat{H}(f) = \frac{G_{xy}(f)}{G_{xx}(f)} \tag{1}$$

Figure 4 schematically shows the procedures used to conduct the analyses discussed herein. After each flight, the flaperon sweeps (input data) and the modal responses (output data) are loaded into the Tilt-Rotor Engineering Database System (TRENDS) for ease of subsequent access. Next, the Frequency Response Identification (FRESPID)[11] program generates the spectral functions from the time histories in TRENDS. Finally, the modal parameters are determined by the curve-fitting program, NAVFIT.[12] All computations are performed off-line (postflight).

Fourier-Transform Computations

The first step is to Fourier-transform the flaperon excitation and structural response data using FRESPID. Flaperon motion is measured by LVDT's; wing responses are measured by separate beam, chord, and torsion strain gages near the wing roots (Fig. 1). Corresponding left and right transducers are summed or differenced, depending on the mode, to form composite inputs and outputs. If the two transducers are properly chosen, then the signals will be highly correlated and in phase for symmetric modes, and highly correlated but reversed in phase for antisymmetric modes. Noise will not be correlated, thereby minimizing corruption of the spectral data.

Figure 5 shows the time histories of one flaperon sweep and the corresponding strain-gage response for the symmetric beam mode. Both signals are the sum of left and right transducer outputs; only symmetric content is visible. The decrease in flaperon amplitude with time, hence frequency, results from limited control-system frequency response. This effect is compensated for during the frequency-response calculations [Eq. (1)].

FRESPID transforms the time-history data to the frequency domain by using a chirp z-transform, which improves on the conventional Cooley-Tukey fast Fourier transform (FTT) by allowing arbitrary resolution over a specified frequency range.[13] The dc components and linear drifts are first removed to prevent oscillation in the spectral calculations. Multiple runs are concatentated to form extended time histories, which are digitally filtered and partitioned into several overlapping sections. Each section is scaled with a cosine weighting function ("Hanning window") to reduce side lobes and leakage.[9] The spectral content of each section is analyzed using the chirp z-transform. The total spectrum is finally determined by averaging the spectra of all of the sections.

Spectral Functions

Once the Fourier coefficients have been computed by the chirp z-transform, the auto- and cross-spectral functions $G_{xx}(f)$, $G_{yy}(f)$, and $G_{xy}(f)$ are calculated by the formulas in Ref. 9, then the frequency response $H(f)$ by Eq. (1). Figure 6 shows the magnitude and phase for the symmetric beam response to flaperon input, plotted in standard Bode form ($\text{dB} = 20 \log_{10} |H(f)|$). The magnitude plot clearly shows a second-order response peak, and the phase plot shows the 90-deg change in phase at the natural frequency.

The coherence function $\gamma^2(f)$ is also computed:

$$\gamma^2(f) = \frac{|G_{xy}(f)|^2}{G_{xx}(f)G_{yy}(f)} \tag{2}$$

For frequency responses, the coherence may be interpreted as that fraction of the output (response) spectrum that is linearly related to the input (excitation) spectrum.[9] If the system is perfectly linear and noise-free, the coherence will be unity. The coherence is a good measure of the quality of the data prior to application of the modal curve fit.

Figure 7 illustrates the coherence function corresponding to the frequency response shown in Fig. 6. Reduced coherence above the natural frequency f_n was seen in all modes, especially near 1/rev (8.6 Hz at 86% rpm). Generally worse coherence was seen in the antisymmetric chord and symmetric torsion modes, falling off significantly at frequencies both above and below f_n. Even so, the coherence was always high enough near the peak response to allow good modal identification.

If adequate direct (flaperon) excitation cannot be achieved, or if there is substantial unmeasurable excitation (turbulence), an alternate method may be useful. In this approach, structural responses from the right and left wings *YR* and *YL* are cross-correlated with each other, rather than with the flaperon inputs. In the symmetric case, the resulting cross-spectrum is

$$G_{YRYL} = |H|^2[G_{xx} + G_{mm}] \tag{3}$$

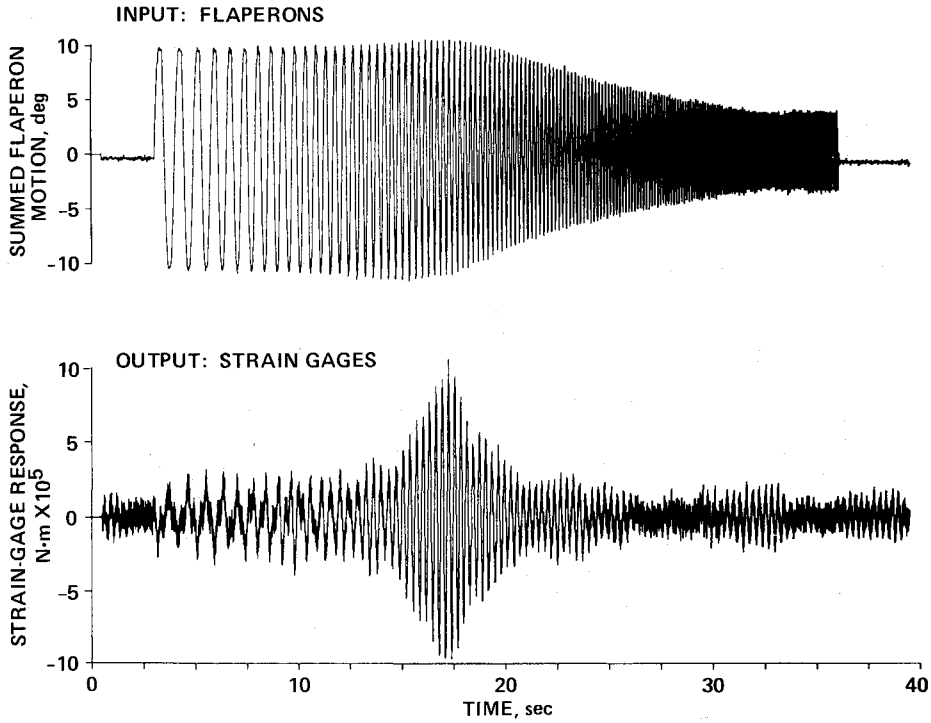

Fig. 5 Input and output time histories for one symmetric flaperon sweep (beam mode).

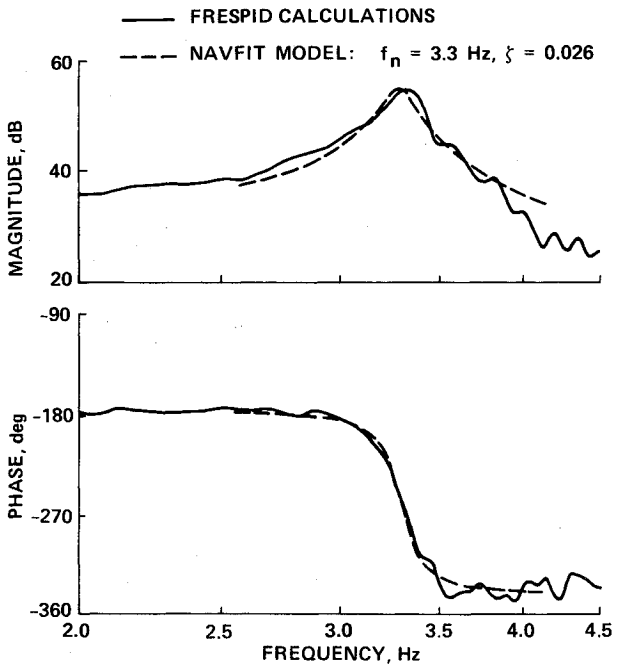

Fig. 6 Symmetric beam mode frequency response and fitted second-order model.

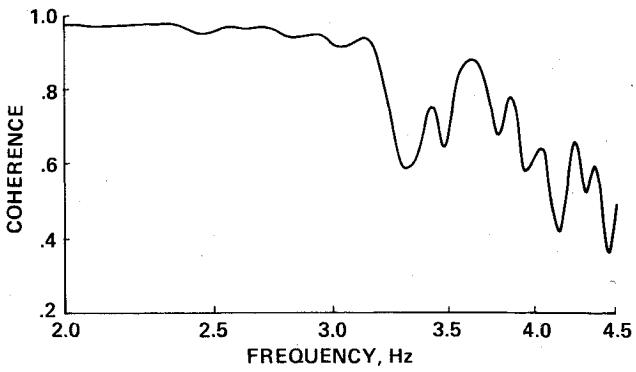

Fig. 7 Coherence function $\gamma^2(f)$ for the symmetric beam mode.

which allows an estimate of the frequency-response magnitude $|H|$ (to within a scale factor, negative for antisymmetric modes) when the total excitation $[G_{xx} + G_{mm}]$ is constant within the frequency range of the modal response. Thus, the (unknown) noise spectrum G_{mm} can be exploited for modal identification when the controllable input spectrum G_{xx} is of inadequate magnitude. The damping ratio and frequency are then determined from the response magnitude estimate alone. This method proved useful in early work, especially for the chord modes.[5] However, the phase information in H is lost; consequently, the full frequency response [Eq. (1)] was used for all results given herein.

Frequency and Damping Calculations

Once frequency responses have been calculated by FRESPID, modal frequencies and damping are determined by curve-fitting the spectral data. Given a structure with natural frequency f_n and damping ratio ζ, the response can be well approximated by a quadratic second-order model of the form

$$H_m(f) = \frac{K}{1 - (f/f_n)^2 + i2\zeta f/f_n} \tag{4}$$

Only such models were used in the present study, as appropriate for structural analysis. (The gain K is determined largely by the sensitivities of the aircraft transducers and has no direct bearing on aeroelastic stability.)

The curve-fitting program NAVFIT is a general multimode, high-order analysis using both magnitude and phase data. The user specifies a frequency range to be fitted and initial estimates of f_n, ζ, and K. Phase shifts caused by unmodeled higher modes or 1/rev are fitted with a time delay. An iterative algorithm systematically varies f_n, ζ, and K to get the best fit, based on 50 frequency points. An example of the use of NAVFIT to determine frequency and damping for the symmetric beam mode is given in Fig. 6; the fitted model is superimposed on the frequency response.

The model is fitted by minimizing a cost function based on the squares of both magnitude and phase errors. The relative weights of the magnitude and phase errors are chosen to yield results equivalent to equal weighting of the real and imaginary parts of the complex frequency response.[11] To emphasize the most reliable data, there is a separate weighting of the errors by an exponential function of the coherence at each frequency point.[14]

In addition to NAVFIT, a method was tried that computed the damping ratio from spectral data by integrating over the spectral peak.[8,15] There were, thus, four possible calculations of frequency and damping: integration and curve fits, each applied to cross spectra and frequency responses. The final choice was based on the scatter in estimating ζ and f_n at the baseline point (defined under Flight-Test Results). NAVFIT applied to frequency responses almost always gave the lowest scatter; even in the exceptional cases, no other method showed any statistically significant improvements.

Flight-Test Results

The frequency sweeps were concentrated within a fairly narrow region of the flight envelope so as to more rigorously verify the frequency-domain technique. The most important data were acquired at 10,000-ft density altitude at 86% rotor speed (8.6 Hz), with a typical gross weight near 13,500 lb. The airspeed range was 180 knots true airspeed (the normal speed for conversion to airplane mode) to 260 knots (the torque-limited maximum speed for level flight).

Limitations on flight-test time did not permit replications of all test points. Therefore, a baseline point of 180 knots at 10,000 ft was chosen as an easily repeatable flight condition to explicitly test for scatter in the frequency and damping estimates.

Earlier flight tests[6] show interaction of the Stability Control Augmentation System (SCAS) with modal responses, which was eliminated by modification of the SCAS. To ensure that there were no other interactions, each part of the automatic flight control system – the SCAS, the Attitude Retention System (ARS), and the Force Feel System (FFS) – was individually turned off during three series of sweeps at the baseline point. In a comparison of the results with the other baseline estimates, no statistically significant differences were noted. These data were subsequently included in the baseline data.

Figure 8 summarizes the frequency and damping results for all six modes. Open symbols are estimates made with exponential-decay methods[16]; closed symbols are frequency-domain estimates. All data are plotted against true airspeed, the critical value for aeroelastics. The frequency-domain method yields low scatter at the baseline point and good consistency between airspeeds, hence higher reliability than the exponential-decay method. (Individual modes are discussed in detail in the following section.)

Numerical results of the frequency-domain method are summarized in Table 1 for the 180-knot baseline point. Listed for each mode are the averages of damping ($\bar{\zeta}$) and frequency ($\bar{f}_n$) and their respective standard deviations (σ_ζ and σ_{fn}). The standard deviations of the damping range from 7 to 9% of the average values, while the standard deviations of the frequency are all less than 1%.

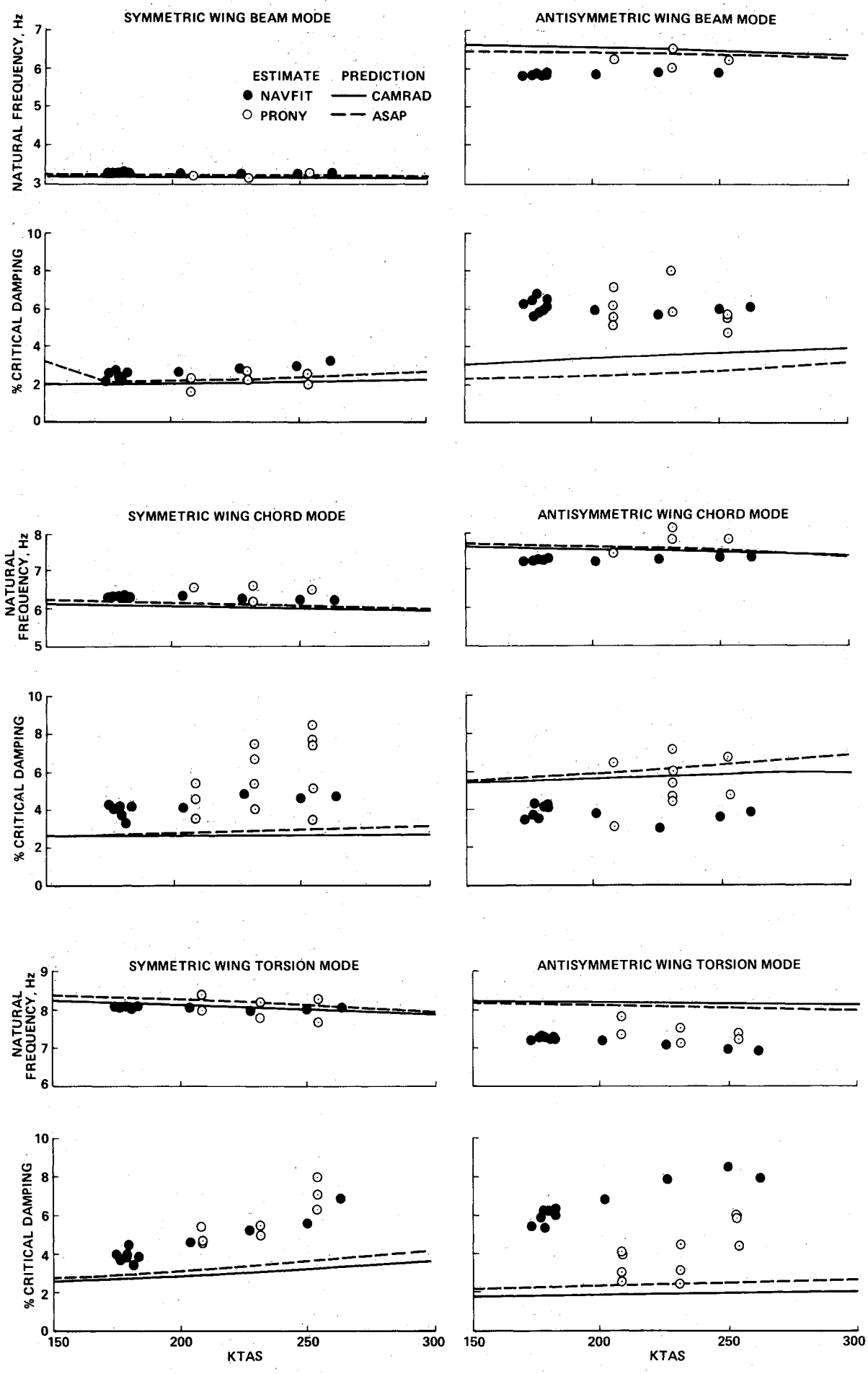

Fig. 8 Summary of XV-15 aeroelastic wing-mode estimates and predictions.

In a few cases – notably, antisymmetric torsion – a statistically significant fraction of the scatter can be explained by weight changes caused by fuel burnoff. It is not practical to collect all flight data at exactly the same fuel state. Therefore, the values given in Table 1 represent realistically achievable performance of the frequency-sweep flight-test method.

Analytical Predictions

A detailed assessment of all available predictive methods is beyond the scope of this paper (see Ref. 17 for a good summary of the development of whirl-mode flutter analyses applying to tilt rotors). Two different programs – ASAP and CAMRAD – were used in order to avoid biasing the comparisons with flight data toward one particular type of analysis. The ASAP and CAMRAD predictions are plotted with the frequency-domain estimates in Fig. 8.

ASAP is a new analysis similar in concept to PASTA,[18] but completely rederived and reprogrammed. The CAMRAD model used here is based on that of Ref. 19, but updated to have the correct precone for the steel hubs plus recalculated NASTRAN mode shapes. The ASAP and CAMRAD predictions were all based on nominal flight-test conditions of 10,000 ft altitude, 86% rotor speed, and 13,000 lb gross weight. (Reference 5 used predictions from DYN4, a less sophisticated program replaced by ASAP, and from an older, less accurate CAMRAD model.) Neither analysis exactly models the aircraft; however, the trends in the results reveal any differences between the two methods.

Both sets of predictions generally agree more closely with each other than with the flight data. All predictions in Fig. 8 were based on identical values of zero-airspeed structural damping (Fig. 2) that were derived from a rotors-off wind tunnel test of an aeroelastic model of the V-22. No comparable data exist for the XV-15 itself that have been directly verified by a structural test. The differences between the ASAP and CAMRAD predictions were generally much less than the differences between the CAMRAD model used here and that of Ref. 5, which used structural damping values from Ref. 20. These results imply that errors in the NASTRAN model of the XV-15 and uncertainties in the estimation of structural damping are at least as important as the differences between ASAP and CAMRAD.

Comparative Statistics

There is no comprehensive set of exponential-decay data corresponding to the frequency-sweep baseline data. In order

Table 1 XV-15 wing modes at the baseline flight condition (statistics are based on 8 data points)

Mode	$\bar{\zeta}$, % critical damping	σ_ζ, % critical damping	σ_ζ, % relative error	$\overline{f_n}$, Hz	σ_{fn}, Hz	σ_{fn}, % relative error
Symmetric beam	2.54	0.235	9.3	3.30	0.0084	0.25
Antisymmetric beam	6.09	0.398	6.5	5.90	0.0424	0.72
Symmetric chord	3.94	0.326	8.3	6.33	0.0110	0.17
Antisymmetric chord	3.89	0.349	9.0	7.25	0.0278	0.38
Symmetric torsion	3.97	0.362	9.1	8.08	0.0205	0.25
Antisymmetric torsion	6.07	0.406	6.7	7.25	0.0396	0.55

Table 2 Statistics for frequency vs airspeed

	Frequency-sweep estimates				Exponential-decay estimates[a]			
Mode	No. of points	Standard error Hz	Intercept, Hz	Slope, Hz/knot $\times 10^{-3}$	No. of points	Standard error, Hz	Intercept Hz	Slope, Hz/knot $\times 10^{-3}$
Symmetric beam	12	0.00965	3.35	−0.265	3	0.0378	2.73	2.49
Antisymmetric beam	12	0.0350	5.67	0.127	4	0.252	6.32	0.00
Symmetric chord	12	0.0159	6.54	−1.18	4	0.212	6.44	0.059
Antisymmetric chord	12	0.0296	7.08	0.893	4	0.289	5.76	10.0
Symmetric torsion	12	0.0324	8.20	−0.684	6	0.298	9.06	−4.84
Antisymmetric torsion	12	0.0397	7.96	−3.98	6	0.248	8.61	−6.05

[a]Data taken from Ref. 16.

Table 3 Statistics for damping vs airspeed

	Frequency-sweep estimates				Exponential-decay estimates[a]			
Mode	No. of points	Standard error, % critical damping	Intercept, % critical damping	Slope % critical damping/ knot, $\times 10^{-3}$	No. of points	Standard error, % critical damping	Intercept, % critcal damping	Slope % critical damping/ knot $\times 10^{-3}$
Symmetric beam	12	0.197	1.13	7.86	6	0.422	0.865	6.86
Antisymmetric beam	12	0.358	6.59	−2.98	9	1.02	8.82	−14.8
Symmetric chord	12	0.307	2.14	10.2	12	1.64	−4.61	50.0
Antisymmetric chord	12	0.373	4.53	−3.85	9	1.64	0.883	21.8
Symmetric torsion	12	0.376	−1.41	30.1	8	0.491	−5.36	55.5
Antisymmetric torsion	12	0.395	0.615	30.8	10	1.01	−5.75	49.2

[a]Data taken from Ref. 16.

to make statistical comparisons between the results of the two flight-test methods, the frequency and damping results were curve-fitted against airspeed. This procedure allows consistent comparisons to be made using all of the data. Linear fits were used, partly because the predictions have nearly constant slopes within the flight-test airspeed range, and partly because the standard error of each fit will be a conservative measure of scatter if the true variations are in fact nonlinear. The curve-fit results are summarized in Tables 2 and 3 for each mode.

Comparing the curve fits, all but one set of frequency-sweep estimates had significantly less scatter (based on a 2.5%-level F-ratio test) in both frequency and damping than the exponential-decay estimates. The one exception was symmetric torsion mode damping; even here, the frequency-sweep method showed less scatter.

The statistical tests indicated in Tables 2 and 3 are potentially misleading because of the small number of data points. Nevertheless, the test are adequate to illustrate that the frequency-domain method is sufficiently sensitive and repeatable to reliably detect a significant decrease in damping should a dangerous part of the flight envelope be entered.

Care should be taken when comparing other published data with the new frequency-sweep results. No complete set of exponential-decay data exists for an aircraft configuration that exactly matches that for the new data. There are two different XV-15 aircraft, on which three different versions of rotor hubs have been flown: titanium hubs with either 2.5- or 1.5-deg precone, and steel hubs with 1.5-deg precone. The frequency-sweep results are for 1.5-deg steel hubs; the exponential-decay results shown here are for 2.5-deg titanium hubs. Other reports on XV-15 aeroelastics (e.g., Refs. 6 and 7) sometimes include data for different configurations of the XV-15, which are thought to have different aeroelastic behavior.

Individual Modes

Symmetric Beam

The new frequency-domain estimates of natural frequency f_n are similar to the old exponential-decay results, and closely follow the predictions. The new estimates of damping ζ increase with airspeed very consistently. The dip in the ASAP predictions of ζ at 175 knots also occurs in the CAMRAD predictions, but at a lower airspeed (not visible in Fig. 8). Otherwise, the differences between the slopes of ASAP and CAMRAD are too small to allow a reliable choice of one over the other.

Antisymmetric Beam

The new estimates of f_n show less scatter than the old estimates and are about 0.5 Hz lower in frequency than the predictions. The new estimates of ζ are much better than the old, but neither set of estimates matches the slope of either predictive method. The estimates are greater than the predictions by a least 0.02 (2% critical damping) in nearly all cases.

Symmetric Chord

The new estimates of f_n are better in scatter than the old, and are about 0.2 Hz above the predictions. The new damping estimates are much improved over the old, but there is still noticeable scatter. The new estimates of ζ are as much as 0.02 higher than predicted and match the CAMRAD slope better than the ASAP slope.

Antisymmetric Chord

The new estimates of f_n are much improved in scatter; they are slightly less than predicted and do not follow the slope of the estimates. The new estimates of ζ show greatly reduced scatter compared to the old and are up to 0.02 less than predicted. The apparent dip in the estimated damping at 225 knots is thought to be caused by scatter.

Symmetric Torsion

The new estimates of f_n are very good and lie within 0.1 Hz of the CAMRAD predictions. They do not show the predicted decrease in f_n as airspeed is increased from the baseline condition. It cannot be determined whether the change in the slope of the estimates above 225 knots is an accurate reflection of XV-15 aeroelastic behavior, or is an illusion caused by scatter. The new estimates of ζ are slightly better than the old, and show significantly faster rise with airspeed than the predictions.

Antisymmetric Torsion

The new estimates of f_n have definitely less scatter than the old. They are generally over 1 Hz lower than the predicted values and decrease more rapidly with airspeed. The new damping estimates are better than the old and have almost twice the magnitude. They also show a steeper slope than the predictions. The new estimates of ζ abruptly decrease at the last, highest-speed point, whereas the old estimates appear to increase in slope. It cannot be determined whether either case reflects a true change in slope or whether both are merely caused by scatter.

Although both antisymmetric chord and antisymmetric torsion, as estimated by NAVFIT, have the same natural frequency at the baseline point (Table 1), the difference between the estimated slopes of the two modal frequencies is statistically significant (Table 2). Furthermore, the damping values for these two modes are clearly different in magnitude and slope (Fig. 8). This shows that the chord and torsion strain gages have low enough crosstalk for the frequency-domain method to resolve two very close modes.

In a few cases, the frequency-domain estimates appear to vary nonlinearly with airspeed, contrary to the roughly linear predictions, but it has not been proven that any such instance indicates a real aeroelastic phenomena. Even at the worst, the overall consistency of the estimates is adequate for reliable determination of aeroelastic modes, which is the goal of this development effort.

Conclusions

Frequency-sweep excitation combined with frequency-domain analysis was demonstrated to be a reliable and efficient way of determining XV-15 aeroelastic behavior from flight data, permitting good estimations of all modes. Dual-flaperon excitation plus sum-and-difference signal processing yielded good time-history data for each mode, and chirp z-transform Fourier analysis generated excellent spectra. Based on curve fits to frequency responses, the estimates of modal frequencies and damping varied linearly with airspeed and were highly repeatable at a reference flight condition (within less than 1% relative error for natural frequency and 9% relative error for damping). Because of the good analytical results shown here, and the reduced flight-test time compared to other methods, the frequency-sweep method has been chosen to support flight test of the new XV-15 composite blades (ATB's), now underway.

Acknowledgments

The authors wish to thank J. R. Gillman of the Boeing Helicopter Corporation for providing upgrades to the CAMRAD model of the XV-15, and S. K Yin of Bell Helicopter Textron for the ASAP predictions.

References

[1]Hall, W. E., "Prop-Rotor Stability at High Advance Ratios," *Journal of the American Helicopter Society*, Vol. 11, April 1966, pp. 11–26.

[2]Edenborough, H. K., "Investigation of Tilt Rotor VTOL Aircraft Rotor-Pylon Stability," *Journal of Aircraft*, Vol. 5, March–April 1968, pp. 97–105.

[3]Popelka, D., Sheffler, M., and Bilger, J., "Correlation of Test

and Analysis for the 1/5 Scale V-22 Aeroelastic Model," *Journal of the American Helicopter Society*, Vol. 32, April 1987, pp. 21-33.

[4]Alexander, H. R., Maisel, M. D., and Giulianetti, D. J., "The Development of Advanced Technology Blades for Tiltrotor Aircraft," Paper No. 39, 11th European Rotorcraft Forum, London, England, Sept. 1985.

[5]Acree, C. W. and Tischler, M. B., "Using Frequency-Domain Methods to Identify XV-15 Aeroelastic Modes," NASA TM-100033, Nov. 1987; and USAAVSCOM TR-87-A-17.

[6]Schroers, L. G., "Dynamic Structural Aeroelastic Stability Testing of the XV-15 Tilt Rotor Research Aircraft," NASA TM-84293, Dec. 1982 and USAAVRADCOM 82-A-17.

[7]Bilger, J. M., Marr, R. L., and Zahedi, A., "In-Flight Structural Dynamic Characteristics of the XV-15 Tilt Rotor Research Aircraft," AIAA Paper 81-0612, Jan. 1981.

[8]Johnson, W., "Development of a Transfer Function Method for Dynamic Stability Measurement," NASA TN D-8522, July 1977.

[9]Bendat, J. S. and Piersol, A. G., *Random Data*, 2nd ed. Wiley and Sons, New York, 1986.

[10]Flanelly, W. G., Fabunmi, J. A., and Nagy, E. J., "Analytical Testing," NASA CR-3429, May 1981.

[11]Tischler, M. B., "Frequency-Response Indentification of XV-15 Tilt-Rotor Aircraft Dynamics," NASA TM-89428, May 1987 and USAAVSCOM TM-87-A-2.

[12]Hodgkinson, J. and Buckley, J., "NAVFIT General Purpose Frequency Response Curve Fit (Arbitrary Order)," McDonnell Aircraft Company, St. Louis, MO, Oct. 1978.

[13]Rabiner, L. R. and Gold, B., *Theory and Application of Digital Signal Processing*, Prentice-Hall, Inc., Englewood Cliffs, NJ, 1975.

[14]Tischler, M. B., "Advancements in Frequency-Domain Methods for Rotorcraft System Identification," Second International Conference On Basic Rotorcraft Research, College Park, MD, Feb. 1988.

[15]Tischler, M. B., Leung, J. G. M., and Dugan, D. C., "Frequency-Domain Identification of XV-15 Tilt-Rotor Aircraft Dynamics," AIAA Paper 83-2695.

[16]Arrington, W. L., Kumpel, M., Marr, R. L., and McEntire, K. G., "XV-15 Tilt Rotor Research Aircraft Flight Test Data Report," NASA CR 177406, June 1985 and USAAVSCOM TR-86-A-1.

[17]Ormiston, R. A., Warmbrodt, W. G., Hodges, D. H., and Peters, D. A., "Rotorcraft Aeroelastic Stability," *NASA/Army Rotorcraft Technology*, NASA CP-2495, Vol. 1, 1988, pp. 353-529.

[18]Kvaternick, R. G., "Studies in Tilt-Rotor VTOL Aircraft Aeroelasticity," Ph.D. Thesis, Case Western Reserve University, Cleveland, OH, June 1973.

[19]Johnson, W. Lau, B. H., and Bowles, J. V., "Calculated Performance, Stability, and Maneuverability of High-Speed Tilting-Prop-Rotor Aircraft," NASA TM-88349, Sept. 1986.

[20]Johnson, W., "An Assessment of the Capability to Calculate Titlting Prop-Rotor Aircraft Peformance, Loads, and Stability," NASA TP-2291, March 1984.